



Influence of Thermophoresis and Brownian Motion on MHD Hybrid Nanofluid MgO - Ag/H₂O Flow along Moving Slim Needle

Chundru Maheswari^{1,*}, Ravuri Mohana Ramana¹, G. Balaji Prakash², D. Ramesh³, D. Vijaya Kumar⁴

¹ Department of Mathematics, Narasaraopeta Engineering College, Narasaraopet, Andhra Pradesh, India

² Department of H&BS, Aditya College of Engineering, Surampalem, East Godavari, Andhra Pradesh, India

³ Department of Engineering Mathematics, College of Engineering, Koneru Lakshmaiah Educational Foundation, Andhra Pradesh, India

⁴ Department of Applied Mathematics, Lakireddy Bali Reddy College of Engineering, Mylavaram, Andhra Pradesh, India

ARTICLE INFO

Article history:

Received 18 September 2023

Received in revised form 27 October 2023

Accepted 8 November 2023

Available online 30 December 2023

Keywords:

Thermophoresis parameter; Brownian motion; MHD hybrid nanofluid; Thin needle; Shooting method

ABSTRACT

The objective of this paper is to analyze the impact of thermophoresis parameter, Brownian motion, velocity ratio parameter, similarity radius of the slim needle, magnetic parameter, Prandtl number and thermal radiation on the steady state, laminar, MHD hybrid nanofluid composed of MgO-Ag/H₂O flowing along a horizontal hot thin needle. To achieve this, the BVP-5C shooting technique is employed through MATLAB to solve the transformed nonlinear ODEs governing the fluid flow. This study investigates the impact of non-dimensional parameters on the flow velocity, temperature and concentration profiles within the hybrid nanofluid. The effects of skin friction, local Nusselt number and Sherwood number are demonstrated through the use of tables. The observation reveals that elevating the thermophoresis parameter results in a simultaneous reduction in the temperature and concentration profiles, while an opposite behavior is observed for Brownian motion. The magnetic parameter and thermal radiation values result in a rising temperature profile, while the trend is reversed for the velocity ratio parameter, Prandtl number and Schmidt number. The Nusselt number demonstrates an upward trend with higher values of thermophoresis parameter, velocity ratio parameter and thermal radiation. Further, Sherwood number experiences an increase with greater values of Brownian motion and magnetic parameter but it displays a contrasting pattern for thermophoresis, velocity ratio parameter and thermal radiation parameter. Validation of this model with existing data has been excellent.

1. Introduction

The measurement of flow velocity, temperature profile and concentration profile are essential for understanding the fluid flow, heat transfer properties and mixing of substances within a flow field [1]. Hybrid nanofluids, which combine nanoparticles with traditional base fluids are widely recognized as superior heat transfer fluids in engineering applications because they significantly enhance heat transfer within the system [2-4]. These fluids exhibit remarkable potential across

* Corresponding author.

E-mail address: cmaheswari2014@gmail.com

<https://doi.org/10.37934/araset.36.2.6790>

various fields, including heat exchange systems, machining coolant, transformer temperature regulation, solar energy collection, micro-scale power generation, nuclear system cooling, efficient heat dissipation, boiling mechanisms, electronic component cooling, refrigeration technologies, drug delivery systems, defence and space and biomedical applications [5].

Magnetohydrodynamics (MHD), also known as magneto-fluid dynamics, investigates the behaviour of electrically conducting fluids within a magnetic field encompassing substances, such as plasmas, electrolytes, saltwater and liquid metals [6,7]. In numerous engineering applications, the incorporation of magnetic fields has the potential to enhance heat transfer processes [8]. Purnima and Upendra [9] conducted an examination of nanofluid behaviour under the influence of a magnetic field considering slip conditions along the boundary layer on a moving surface. Dharmamah *et al.*, [10] studied the impact of a stretched sheet on the blood flow of a Casson ferromagnetic fluid. Heat dissipation characteristics of a layered stretched sheet in an MHD mixed convective Eyring-Powell fluid flow were investigated by Bharatkumar *et al.*, [11]. Madhura *et al.*, [12] studied the effect of heat and mass transfer on mixed convective nanofluid flow, while Sarfraz and Khan [13] investigated the same in planar and axisymmetric ternary hybrid nanofluid flows. Sarfraz and Khan [14] investigated the impact of a magnetic field on the flow of a hybrid nanofluid containing graphene oxide (GO) and cobalt oxide (Co_3O_4) nanoparticles past a biaxially stretched surface. In another study [15], the same authors determined the asymptotic behaviour of the flow for low and high magnetic numbers.

Thermal radiation plays a crucial role in surface heat transfer processes, especially in situations where convection's heat transfer coefficient is at its lowest [16]. The impact of thermal radiation on the flow of an MHD fractional Oldroyd-B nanofluid in a porous medium was investigated by Babitha *et al.*, [17]. In [18], Anitha *et al.*, investigate the thermal characteristics of a tangent hyperbolic fluid as it flows through a vertical micro channel. Sarfraz and Khan [19] conducted an investigation into the entropy generation analysis of nanofluid flows containing carbon nanotubes (CNTs) driven by the motion of a solid plate. Guled *et al.*, [20] conducted research on the impact of MHD slip flow with radiation, suction/injection on heat transfer over a shrinking sheet. They employed the HAM in their study.

The investigation of the flow characteristics around a thin needle has garnered significant attention among researchers due to its significance in various industrial sectors including hot wire anemometer, electronic devices, plastic sheet extrusion, production of geothermal energy and wire coating [21]. The slender needle is considered to be a body of revolution whose thickness is smaller than the boundary layer [22]. It also plays a significant role in various industrial domains like engineering, medicine, blood flow complications, encompassing lubrication, dynamics of smart coating manufacturing, wind forecasting and transportation [23]. Lee was the first to investigate the flow of momentum boundary layer around a slender needle within a fluid with viscosity [24]. Lee's findings revealed that as the thickness of the needle tends to zero, the displacement and drag per unit of length experience a gradual reduction, eventually converging to zero as the needle diminishes in size. Subsequently, Narain and Uberoi [25-27] expanded upon Lee's work by exploring the effects of forced, free and mixed convection flows in this context. Following their pioneering contributions, numerous researchers have actively engaged in studying and solving the intricate challenges posed by boundary layer flows over slender needles.

In research conducted by Dinarvand *et al.*, [28], an investigation was carried out on the impact of thermal radiation on a steady state, laminar, $\text{MgO} - \text{Ag}/\text{H}_2\text{O}$ MHD flow along a horizontal thin needle. The finite difference method was employed for analysis and intriguingly the authors revealed the existence of dual solutions. Through an extensive stability analysis, the researchers demonstrated that the first solutions consistently remained physically stable throughout the study. Iskander *et al.*,

[29] conducted a study to explore the impact of resistive heating on a continuously moving slender needle immersed in a Sakiadis Ti-Cu/water-ethylene glycol hybrid nanofluid. Sultana *et al.*, [30] investigated solar radiation, dissipative heat transport impacts on a steady mixed convective hybrid nanofluid flow system considering a non-compressible fluid past a moving slender needle. In a scholarly investigation, Iskandar *et al.*, [31] delved into the realm of steady state, mixed convective hybrid nanofluid flow fast over a vertical slender needle as a factor of interest.

Thermophoresis and Brownian motion are two key parameters that significantly influence the characteristics of hybrid nanofluids. Thermophoresis, characterized by the migration of particles from areas of elevated temperature to the regions of lesser temperature is invaluable for particle accumulation such as the transport of electrical charge carriers in semiconductors [32,33]. Brownian motion refers to the erratic motion exhibited by particles suspended in a fluid arising from their interactions with the surrounding fluid molecules. The phenomenon of Brownian motion drives particle migration from regions of greater concentration to regions of lesser concentration [34]. The enhanced heat transfer properties of these two parameters render them highly applicable across diverse uses encompassing electronic cooling, heat exchangers, aerosol technology, solar accumulators, silicon thin film deposition and heat exchanger corrosion [35,36]. Almeida *et al.*, [37] explored the intricate characteristics of micropolar fluids in micro channels considering the effects of Brownian motion and thermophoresis. Madhura and Babitha [38] conducted a study to examine the impact of nonlinear thermal radiation on the unsteady boundary layer flow of a micropolar Carreau nanofluid along a stretching sheet in the presence of Brownian motion and thermophoresis. Their investigation utilized the finite difference method to analyse the problem. Raheem *et al.*, [39] conducted a study to explore the influence of thermophoresis and Brownian diffusion on the flow behaviour of a rotating three-dimensional Ag – CuO/H₂O hybrid nanofluid over a linearly stretched sheet.

Madhukesh *et al.*, [40] investigated the impact of thermophoresis parameter within a hybrid nanofluid flow over a slender rotating needle. Iskandar [41] conducted a study to examine how Brownian motion and thermophoresis affect the Cu – Al₂O₃/H₂O flow past a permeable moving slim needle utilizing the finite difference method as the investigative approach. Sultana [42] investigated the stable, non-compressible boundary layer flow and transfer of heat around a mobile slender needle soaked in Al₂O₃ – Cu/H₂O considering influential factors such as solar radiation, viscous dissipation, thermophoresis, Brownian motion and the researcher employed the MAPLE software scheme for numerical solutions and result analysis. Arshad *et al.*, [43] investigated the heat transmission distribution in Ag – CuO/H₂O flow along a horizontally positioned hot slim needle. The investigation encompassed various influential factors, including hall current, thermophoresis, Brownian motion, chemical reaction and viscous dissipation within the system. They employed the HAM technique to successfully derive a solution for the formulated problem. The same authors in [44] conducted thermal analysis on a bio-convective Cu – Al₂O₃/H₂O flow over a slender needle that was moving horizontally. The study incorporates considerations for viscous dissipation and chemical reaction taking into account the existence of microorganisms. To mathematically describe the phenomena of flow the widely acknowledged Buongiorno's model was employed. Additionally, the study explored the influence of Brownian motion and thermophoretic forces on the flow structure using the Homotopy Analysis Method.

Upon reviewing the aforementioned literature, it becomes evident that prior studies have not addressed the combined effects of thermophoresis parameter and Brownian motion on the flow characteristics of a laminar, steady, MHD MgO – Ag/H₂O hybrid nanofluid along a horizontal hot thin needle using the shooting technique. The novelty of this study lies in investigating the application of an MHD hybrid nanofluid, specifically MgO – Ag/H₂O, in the context of laminar and steady-state

flow over a horizontally oriented thin needle capable of moving either in the same or opposite direction as the free stream by using the shooting method. The impacts of thermophoresis parameter and Brownian motion are also considered. BVP-5C shooting technique in MATLAB was implemented to numerically solve the transformed nonlinear ODEs. The investigation explores the impacts of several non-dimensional parameters like thermophoresis, Brownian motion, velocity ratio parameter, similarity radius of the slim needle, magnetic parameter, Prandtl number, Schmidt number and thermal radiation on velocity, temperature and concentration distributions. The skin friction coefficient, local Nusselt number and local Sherwood number are presented in tabular form. The obtained results demonstrate a strong concurrence with the existing literature. The findings of this research could be applied to the development of hot wire anemometers, micro scale cooling devices, shielded thermocouples for wind velocity measurement, solar collectors, heat exchangers and microstructure electronic devices with high compact and effectiveness [45].

2. Mathematical Formulation

In this investigation, we consider a steady state, laminar, axisymmetric MHD boundary layer stream with the impacts of thermophoresis parameter and Brownian motion occurring around a heated slender needle that moves horizontally and continuously filled with a MgO – Ag/H₂O defined by Esfe *et al.*, [46] as shown in Figure 1.

In this context, the variables x and r represent the cylindrical coordinates, where x denotes the axial coordinate and r corresponds to the radial coordinate. The needles that we consider are only those whose thickness is similar to or smaller than that of the boundary layer. Free stream velocity U_∞ , velocity of needle u_w , ambient temperature T_∞ and the hot needle temperature T_w are constants. Also, the direction of the free stream velocity is continuously moving towards the right. In the context of the slim needle estimation, the influence of pressure gradient along the needle is considered negligible [47]. According to our single-phase model, there exists thermal equilibrium between the base fluid and nanoparticles and no discernible slip is observed between the two phases. The selected hybrid nanofluid MgO – Ag/H₂O is prepared by dispersing Magnesium oxide (MgO) inside the base fluid water followed by Silver (Ag) with a high thermal conductivity.

Considering the aforementioned assumptions and utilization of the Tiwari-Das model [48] along with the Roseland approximation [49], the governing set of non-linear PDEs encompassing continuity, momentum, energy and concentration equations can be expressed as follows (from Dinarvand [28]):

$$\frac{\partial}{\partial x}(ru) + \frac{\partial}{\partial r}(rv) = 0 \quad (1)$$

$$u \frac{\partial u}{\partial x} + v \frac{\partial u}{\partial r} = \frac{\mu_{hnf}}{\rho_{hnf}} \frac{1}{r} \frac{\partial}{\partial r} \left(r \frac{\partial u}{\partial r} \right) - \frac{\sigma B_0^2 u}{\rho_{hnf}} \quad (2)$$

$$u \frac{\partial T}{\partial x} + v \frac{\partial T}{\partial r} = \frac{1}{(\rho C_p)_{hnf}} \left[\frac{16\sigma^* T_\infty^3}{3K^*} + k_{hnf} \right] \frac{1}{r} \frac{\partial}{\partial r} \left(r \frac{\partial T}{\partial r} \right) + \tau \left[D_B \frac{\partial C}{\partial r} \frac{\partial T}{\partial r} + \frac{D_T}{T_\infty} \left(\frac{\partial T}{\partial r} \right)^2 \right] \quad (3)$$

$$u \frac{\partial C}{\partial x} + v \frac{\partial C}{\partial r} = \frac{D_B}{r} \frac{\partial}{\partial r} \left(r \frac{\partial C}{\partial r} \right) + \frac{D_T}{T_\infty} \frac{1}{r} \frac{\partial}{\partial r} \left(r \frac{\partial T}{\partial r} \right) \quad (4)$$

According to the above-mentioned assumptions, the provided boundary conditions are:

$$u = u_w, v = 0, T = T_w, D_B \frac{\partial C}{\partial r} + \frac{D_T}{T_\infty} \frac{\partial T}{\partial r} = 0 \text{ at } r = R(x),$$

$$u \rightarrow U_\infty, T \rightarrow T_\infty, C \rightarrow C_\infty \text{ as } r \rightarrow \infty. \tag{5}$$

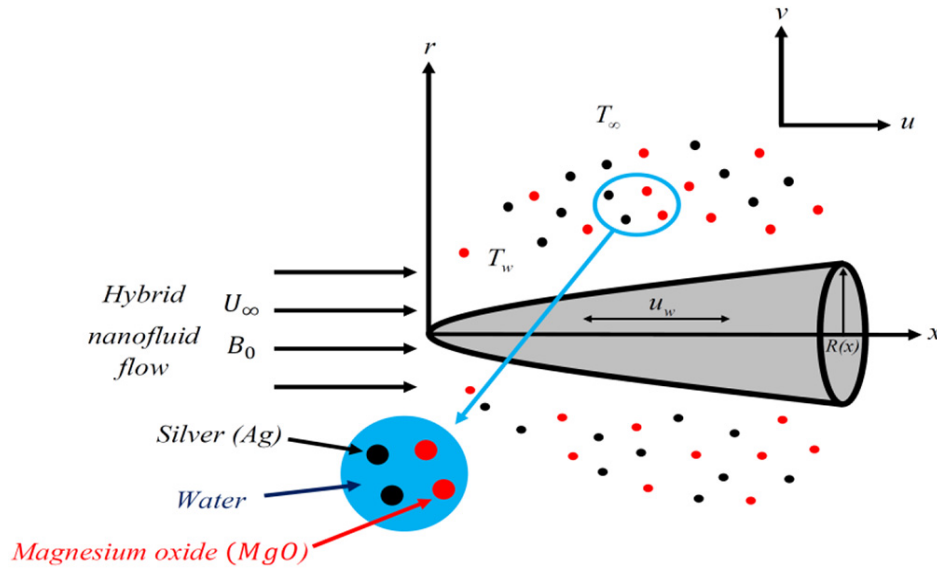


Fig. 1. Geometry of the flow problem [28]

While considering the static part, MgO and Ag nano particles volume fractions ϕ_1, ϕ_2 and equivalent volume fraction of nanoparticles ϕ_e are defined as [28]:

$$\phi_1 = \frac{\frac{m_1}{\rho_1}}{\frac{m_1}{\rho_1} + \frac{m_2}{\rho_2} + \frac{m_f}{\rho_f}}, \quad \phi_2 = \frac{\frac{m_2}{\rho_2}}{\frac{m_1}{\rho_1} + \frac{m_2}{\rho_2} + \frac{m_f}{\rho_f}}, \quad \phi_e = \phi_1 + \phi_2. \tag{6}$$

The viscosity μ_{hnf} , density ρ_{hnf} , thermal conductivity k_{hnf} , heat capacity $(\rho C_p)_{hnf}$ for hybrid nanofluids, which are related to each other, are defined as shown in Table 1.

Table 1

Relevant thermos physical characteristics suggested for MgO – Ag/H₂O hybrid Nanofluid [50-52]

Properties	MgO – Ag/H ₂ O hybrid nanofluid
Viscosity (μ)	$\mu_{hnf} = \frac{\mu_f}{(1 - \phi_e)^{2.5}}$
Density (ρ)	$\rho_{hnf} = (1 - \phi_e)\rho_f + \phi_e\rho_s$, where $\rho_s = \frac{\rho_1 m_1 + \rho_2 m_2}{m_1 + m_2}$
Thermal conductivity (k)	$\frac{k_{hnf}}{k_{nf}} = \frac{k_2 + 2k_{nf} - 2\phi_2(k_{nf} - k_2)}{k_2 + 2k_{nf} + \phi_2(k_{nf} - k_2)}$, where $\frac{k_{nf}}{k_f} = \frac{k_1 + 2k_f - 2\phi_1(k_f - k_1)}{k_1 + 2k_f + \phi_1(k_f - k_1)}$
Heat capacity (ρC_p)	$(\rho C_p)_{hnf} = (1 - \phi_e)(\rho C_p)_f + \phi_e(\rho C_p)_s$, where $(C_p)_s = \frac{(C_p)_1 m_1 + (C_p)_2 m_2}{m_1 + m_2}$

3. Method of Transformation

As proposed by Lee [24], the aforementioned problem can be simplified by incorporating the subsequent similarity variables:

$$\eta = \frac{U_0 r^2}{v_f x}, \psi = v_f x f(\eta), u = \frac{1}{r} \frac{\partial \psi}{\partial r} = 2U_0 f'(\eta), v = -\frac{1}{r} \frac{\partial \psi}{\partial x} = \frac{U_0 r f'(\eta)}{x} - \frac{v_f f(\eta)}{r},$$

$$\theta(\eta) = \frac{T - T_\infty}{T_w - T_\infty}, \phi(\eta) = \frac{C - C_\infty}{C_w - C_\infty}. \quad (7)$$

Following are the non-dimensional parameters

$$M = \frac{\sigma B_0^2 x}{2\rho_f U_0}, R = \frac{16\sigma^* T_\infty^3}{3K^* k_f}, Pr = \frac{v_f (\rho C_p)_f}{k_f}, D_T = \frac{Nt v_f T_\infty}{\tau(T_w - T_\infty)}, D_B = \frac{Nb v_f}{\tau(C_w - C_\infty)}, Sc = \frac{v_f}{D_B}$$

$$c = \frac{U_0 R(x)^2}{v_f x}, \lambda = \frac{u_w}{U_0}. \quad (8)$$

Where $U_0 = u_w + U_\infty$ is the sum of velocity of free stream and the thin needle. The Tiwari-Das [48] model for nanofluids is used when PDEs thermophysical properties correlated to hybrid nanofluids and their similarity variable properties correspond to base fluids. Using thermophysical properties of hybrid nanofluids given in Table 1, the similarity transformations given in Eq. (7) and the non-dimensional parameters given in Eq. (8), Eq. (2) to Eq. (4) becomes

$$2A_1(\eta f'''' + f'') + A_2 f f'' - M f' = 0 \quad (9)$$

$$2\left(R + \frac{k_{hnf}}{k_f}\right)(\eta \theta'' + \theta') + A_3 Pr (f \theta' + 2\eta(Nb \theta' \phi^1 + Nt \theta'^2)) = 0 \quad (10)$$

$$2(\eta \phi'' + \phi') + 2 \frac{Nt}{Nb} (\eta \theta'' + \theta') + Sc f \phi' = 0 \quad (11)$$

Where $A_1 = \left(1 - \frac{\frac{m_1 + m_2}{\rho_1 + \rho_2}}{\frac{m_1 + m_2 + m_f}{\rho_1 + \rho_2 + \rho_f}}\right)^{-2.5}$, $A_2 = 1 - \frac{\frac{m_1 + m_2}{\rho_1 + \rho_2}}{\frac{m_1 + m_2 + m_f}{\rho_1 + \rho_2 + \rho_f}} + \frac{\frac{m_1 + m_2}{\rho_1 + \rho_2}}{\frac{m_1 + m_2 + m_f}{\rho_1 + \rho_2 + \rho_f}} \frac{\rho_s}{\rho_f}$, $A_3 = 1 - \frac{\frac{m_1 + m_2}{\rho_1 + \rho_2}}{\frac{m_1 + m_2 + m_f}{\rho_1 + \rho_2 + \rho_f}} + \frac{\frac{m_1 + m_2}{\rho_1 + \rho_2}}{\frac{m_1 + m_2 + m_f}{\rho_1 + \rho_2 + \rho_f}} \frac{(\rho C_p)_s}{(\rho C_p)_f}$.

Putting the similarity transformations given in Eq. (7) into Eq. (5) will give the following boundary conditions:

$$f(c) = \frac{c\lambda}{2}, f'(c) = \frac{\lambda}{2}, \theta(c) = 1, Nb\phi'(c) + Nt\theta'(c) = 0$$

$$f'(\infty) \rightarrow \frac{1-\lambda}{2}, \theta(\infty) \rightarrow 0, \phi(\infty) \rightarrow 0 \quad (12)$$

Thermophoresis parameter Nt , Brownian motion Nb , magnetic parameter M , Prandtl number (Pr), radiation parameter R , Schmidt number Sc , velocity ratio parameter λ , similarity radius of the slim needle c are the important parameters in the above BVP given in Eq. (9) to Eq. (12). To obtain the needle radius function as $R(x) = \left(\frac{v_f c x}{U_0}\right)^{0.5}$, the value of $\eta = c$ is considered. Furthermore, the parameter $\lambda = \frac{u_w}{U_0}$ holds significant significance in the analysis of flow systems which is interpreted as follows:

- i. when $\lambda = 0$, the fluid is in motion, while the needle remains stationary
- ii. when $\lambda = 1$, the fluid is stationary, while the needle is in motion

- iii. when $0 < \lambda < 1$, both the fluid and the needle exhibit motion in the direction of positive x -axis
- iv. when $\lambda < 0$, the fluid exhibit motion in the direction of positive x -axis, whereas the needle exhibit motion in the direction of negative x -axis. In this study, we specifically focus on the scenario where $\lambda < 0$, signifying the fluid's motion towards the positive x -axis, while the needle moves in the direction of negative x -axis.

Interested physical quantities in this problem are skin friction coefficient (C_f), local Nusselt number (Nu_x) both as defined in Hashim *et al.*, [53], and the Sherwood number Sh_x defined as in Iskandar *et al.*, [41] are given by:

$$C_f = \frac{\tau_w}{\rho_f U_0^2}, Nu_x = \frac{xq_w}{k_f(T_w - T_\infty)}, Sh_x = \frac{xq_m}{D_B(C_w - C_\infty)} \quad (13)$$

$$\text{Where, } \tau_w = \mu_{hnf} \left(\frac{\partial u}{\partial r} \right)_{r=R(x)}, q_w = -k_{hnf} \left(\frac{\partial T}{\partial r} \right)_{r=R(x)}, q_m = -D_B \left(\frac{\partial C}{\partial r} \right)_{r=R(x)} \quad (14)$$

Substituting Eq. (7) and Eq. (14) in Eq. (13), we get

$$\begin{aligned} (Re_x)^{0.5} C_f &= 4c^{0.5} A_1 f''(c), (Re_x)^{-0.5} Nu_x = -2c^{0.5} \frac{k_{hnf}}{k_f} \theta'(c) \\ (Re_x)^{-0.5} Sh_x &= -2c^{0.5} \phi'(c). \end{aligned} \quad (15)$$

Where Re is defined as $Re = \frac{U_0 x}{\nu_f}$.

4. Method of Solution

First, express the ODEs given in Eq. (9) to Eq. (11) in the following form for the transition:

$$f''' = \frac{1}{2A_1 \eta} (-2A_1 f'' - A_2 f f'' + M f') \quad (16)$$

$$\theta'' = \frac{-A_3 Pr f \theta' - 2 \left(R + \frac{k_{hnf}}{k_f} \right) \theta' - 2\eta A_3 Pr (Nb \theta' \phi' + Nt \theta'^2)}{2\eta \left(R + \frac{k_{hnf}}{k_f} \right)} \quad (17)$$

$$\phi'' = \frac{-2Nt \left(\frac{-A_3 Pr f \theta' - 2 \left(R + \frac{k_{hnf}}{k_f} \right) \theta' - 2\eta A_3 Pr (Nb \theta' \phi' + Nt \theta'^2)}{2 \left(R + \frac{k_{hnf}}{k_f} \right)} + \theta' \right) - Nb Sc f \phi' - 2Nb \phi'}{2\eta Nb} \quad (18)$$

These equations are non-linear and does not have an analytical solution. They are solved numerically using RK method with BVP-5C shooting technique through user friendly software MATLAB. In this procedure, firstly the above Eq. (16) to Eq. (18) accompanied with boundary conditions are reduced to seven first order equations. Suitable initial estimations are employed to fulfil the asymptotic boundary conditions given in Eq. (12). We choose

$$f = y(1), f' = y(2), f'' = y(3), \theta = y(4), \theta' = y(5), \phi = y(6), \phi' = y(7). \quad (19)$$

As a result, Eq. (16) to Eq. (18) reduces to

$$f''' = \frac{1}{2A_1\eta} (-2A_1y(3) - A_2y(1)y(3) + My(2)) \quad (20)$$

$$\theta'' = \frac{-A_3Pr y(1)y(5) - 2\left(R + \frac{k_{hnf}}{k_f}\right)y(5) - 2\eta A_3Pr(Nby(5)y(7) + Nty(5)^2)}{2\eta\left(R + \frac{k_{hnf}}{k_f}\right)} \quad (21)$$

$$\phi'' = \frac{-2Nt\left(\frac{-A_3Pr y(1)y(5) - 2\eta\left(R + \frac{k_{hnf}}{k_f}\right)y(5) - 2\eta A_3Pr(Nby(5)y(7) + Nty(5)^2)}{2\left(R + \frac{k_{hnf}}{k_f}\right)} + y(5)\right) - NbScy(1)y(7) - 2Nby(7)}{2\eta Nb} \quad (22)$$

With the boundary conditions

$$\begin{aligned} ya(1) &= \frac{c\lambda}{2}, ya(2) = \frac{\lambda}{2}, ya(4) = 1, Nbya(7) + Ntya(5) = 0, \\ yb(2) &= \frac{1-\lambda}{2}, yb(4) = 0, yb(6) = 0 \end{aligned} \quad (23)$$

Where ya and yb represent the functions corresponding to their respective dependent variables evaluated at $\eta = c$ and $\eta = \infty$ resp. The BVP-5C yields a solution that exhibits continuity over the interval $[c, \infty]$ and maintains a continuous first derivative within this domain. Now, Eq. (20) to Eq. (23) are coded in MATLAB software and their solutions are obtained by the BVP-5C solver. The approach commences with an initial estimation provided at the starting grid points and dynamically adjusts the step size to achieve the desired level of precision. The ultimate count of grid points is determined iteratively by the BVP-5C solver as it progresses through the solution. In Table 2, the governing parameters that determine the solution are listed. The results obtained in this study demonstrate the influence of dimensionless parameters, including thermophoresis parameter, Brownian motion, velocity ratio parameter, slim needle's similarity radius, magnetic parameter, Prandtl number and thermal radiation on flow velocity, temperature, concentration, skin friction coefficient, Nusselt number and Sherwood number. The solution's accuracy rate is 10^{-6} .

Table 2
 MgO, Ag and H₂O thermo physical properties [54,55]

Properties	MgO	Ag	H ₂ O
ρ	3580	10500	997.1
C_p	879	235	4179
k	30	429	0.613
Particle size (in nanometers)	40	2-5	-
Pr			6.2

5. Results and Discussion

The primary objective of this investigation is to explore the utilization of a hybrid nanofluid, namely MgO – Ag/H₂O, within a laminar steady state MHD flow. This flow occurs along a horizontal slender needle capable of moving in either the same or opposite direction as the free stream. The study further examines the influence of thermophoresis parameter and Brownian motion on the

system. MgO nanoparticles with volume fraction ϕ_1 is dispersed in the base fluid H₂O to produce MgO – H₂O nanofluid. To evolve the destination MgO – Ag/H₂O hybrid nanofluid, silver with volume fraction ϕ_2 is distributed into MgO – H₂O nanofluid. The resultant ODEs given in Eq. (9) to Eq. (11) subject to the related boundary conditions of Eq. (12) are solved by using BVP-5C shooting technique via MATLAB. Furthermore, the effect of governing parameters including thermophoresis, Brownian motion, velocity ratio parameter, slim needle's similarity radius, magnetic parameter, Prandtl number, thermal radiation and Schmidt number are portrayed and discussed.

Thermophoresis parameter (Nt) exerts a substantial influence on both temperature profile $\theta(\eta)$ and concentration distribution $\phi(\eta)$ of MgO – Ag/H₂O hybrid nanofluid, as shown in Figures 2 and 3. An increase in Nt results in a decrease in temperature profile and concentration distributions, because the thermophoretic force becomes stronger, causing more particles to move from hotter regions to colder regions. This also increases the hybrid nanofluid's thermal conductivity, which allows it to penetrate deeper into the nanoparticles and reduce the concentric boundary layer thickness. As a result, the concentration characteristics decrease.

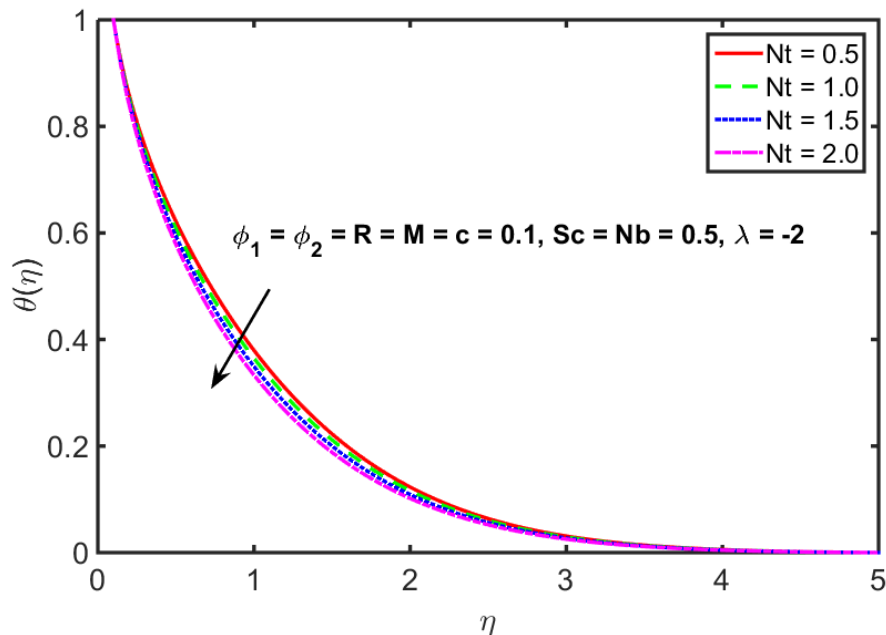


Fig. 2. Nature of $\theta(\eta)$ for Nt

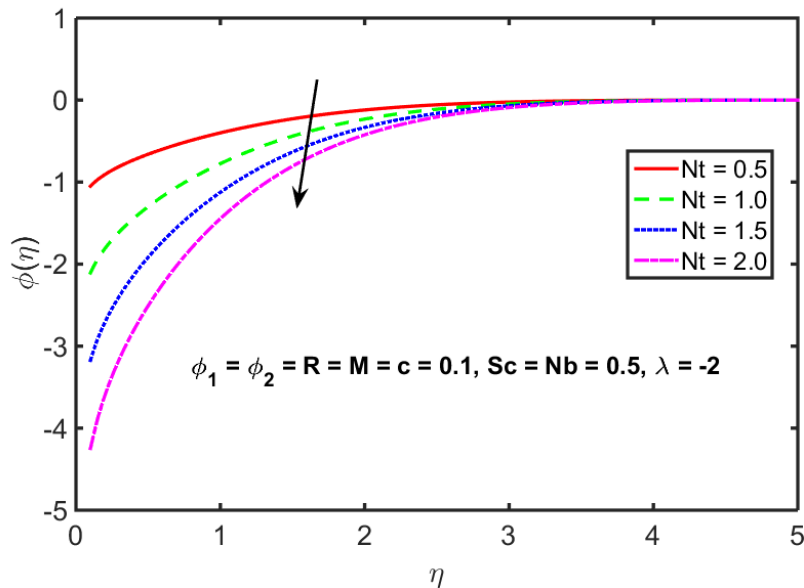


Fig. 3. Nature of $\phi(\eta)$ for Nt

As the Brownian motion Nb increases, nanoparticles random motion increases, leading to more collisions between nanoparticles. This collisional transfer of kinetic energy from the nanoparticles to the fluid increases the thickness of the thermal boundary layer, which in turn increases the profile of temperature $\theta(\eta)$ as shown in Figure 4.

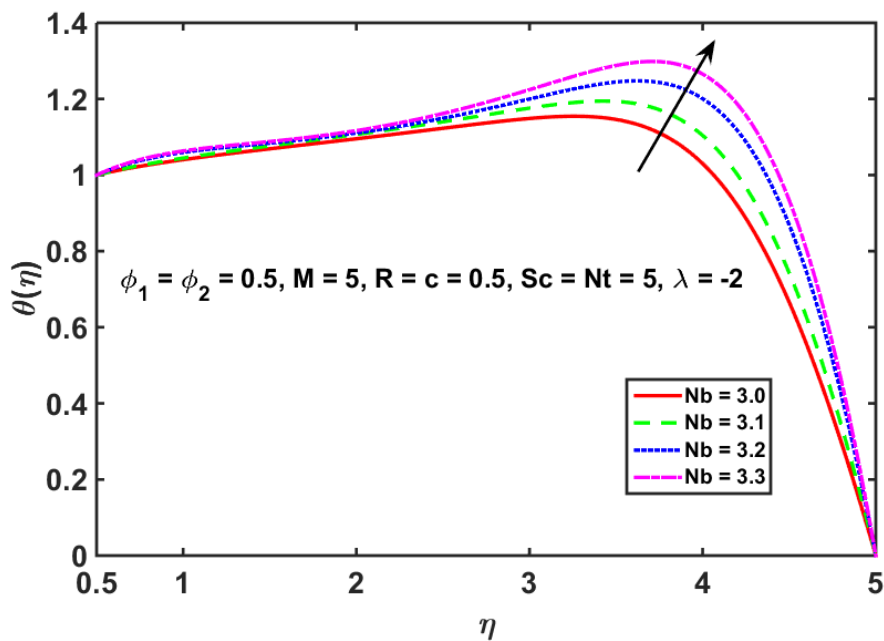


Fig. 4. Nature of $\theta(\eta)$ for Nb

As Nb increases, the rate of mass transfer decreases, which increases the boundary layer thickness of the hybrid nanofluid. This results in a higher concentration profile $\phi(\eta)$ as shown in Figure 5.

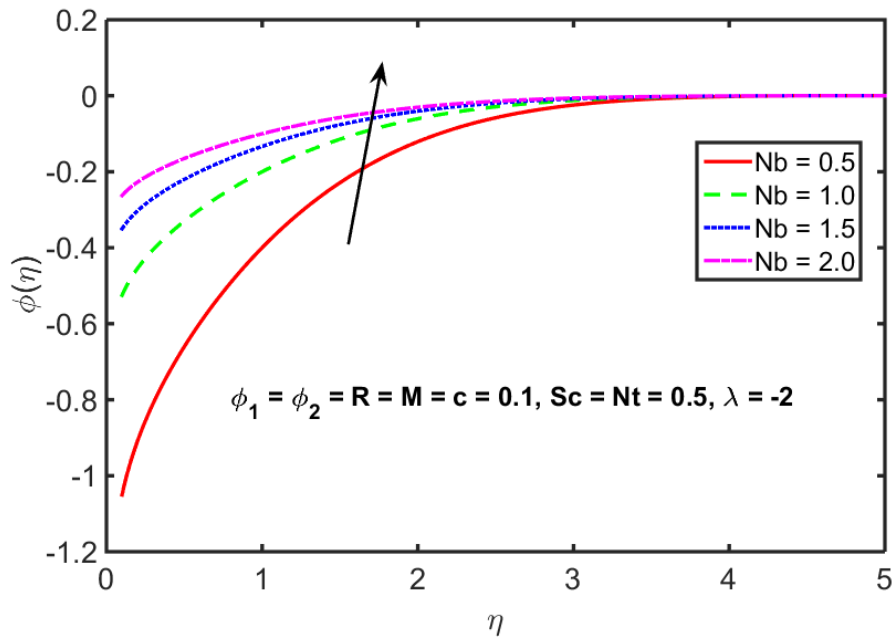


Fig. 5. Nature of $\phi(\eta)$ for Nb

The parameter λ , known as the velocity ratio, exerts a considerable influence on the profiles of $f'(\eta)$, $\theta(\eta)$ and $\phi(\eta)$ for MgO – Ag/H₂O hybrid nanofluid, as illustrated in Figures 6 to 9. When $\lambda < 0$, an interesting duality in the velocity profile is evident. As λ is elevated, the velocity profile in the vicinity of the slim needle progressively amplifies, whereas it diminishes as moves farther away from the needle as shown in Figure 6.

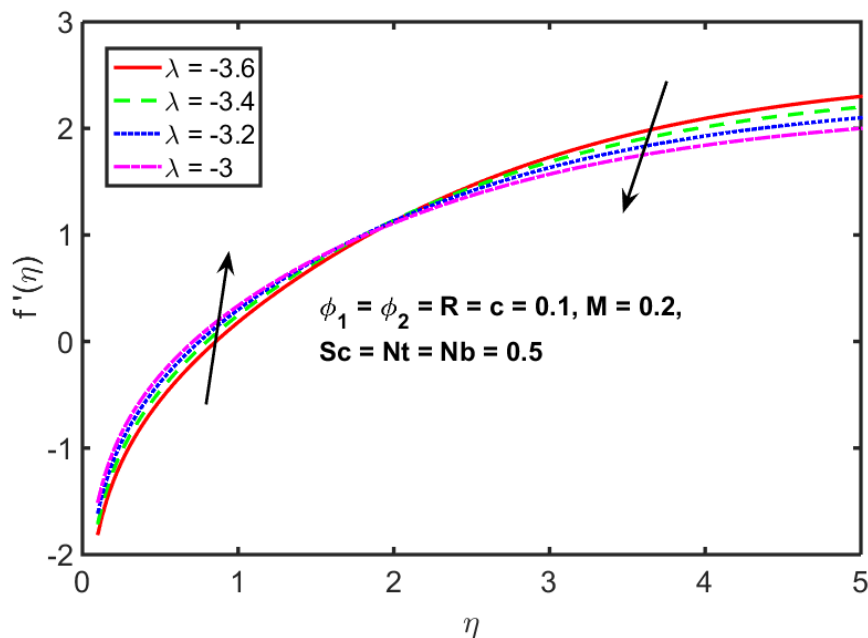


Fig. 6. Nature of $f'(\eta)$ for $\lambda < 0$

However, for $0 \leq \lambda \leq 1$, a distinct trend emerges, showing a decreasing velocity profile as depicted in Figure 7. An increase in λ leads to improved thermal conductivity, convective heat transfer and fluid mixing.

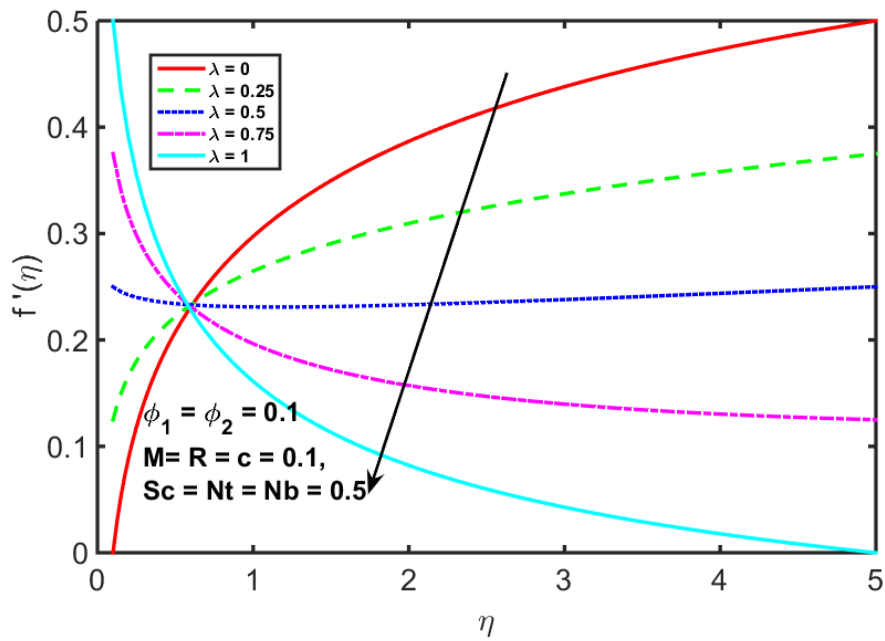


Fig. 7. Nature of $f'(\eta)$ for $0 \leq \lambda \leq 1$

These improvements result in a more efficient heat transfer process, which is evidenced by a decrease in $\theta(\eta)$ as shown in Figure 8.

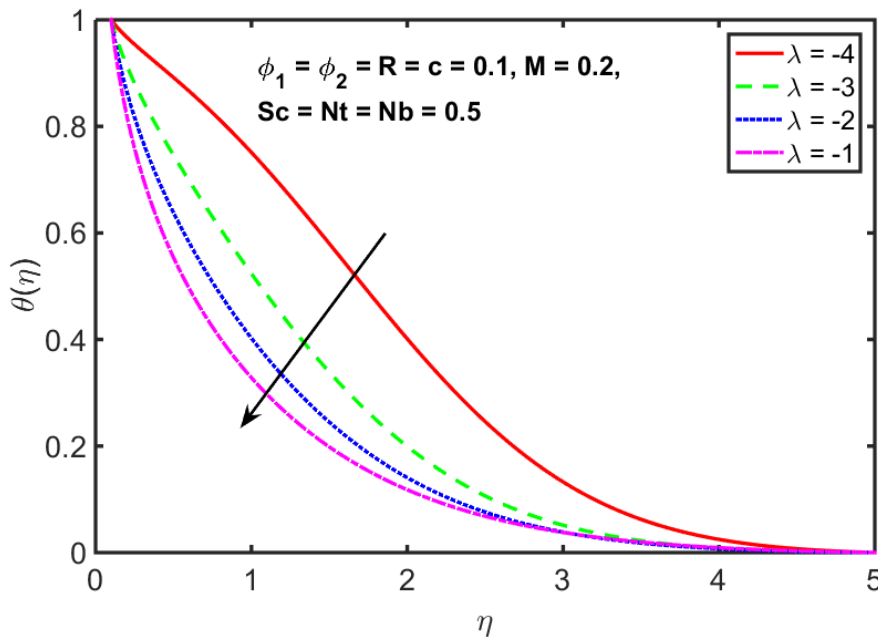


Fig. 8. Nature of $\theta(\eta)$ for λ

Figure 9 shows that an increase in λ causes the nanoparticles velocity to increase relative to the base fluid. This nanoparticles dispersion throughout the fluid leads to an upsurge in the concentration profile.

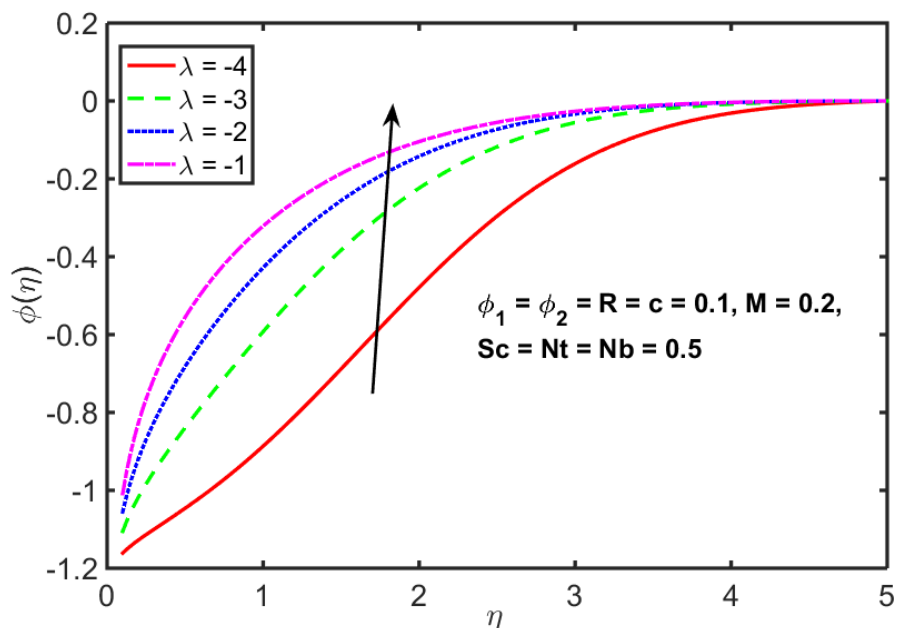


Fig. 9. Nature of $\phi(\eta)$ for λ

Figures 10 to 12 illustrate the influence of the needle's similarity radius (c) on $f'(\eta)$, $\theta(\eta)$ and $\phi(\eta)$ concerning MgO – Ag/H₂O hybrid nanofluid. Increasing the radius of the needle leads to a decrease in $f'(\eta)$ and $\phi(\eta)$, whereas an inverse pattern is observed for $\theta(\eta)$. Physically, increasing the radius of the needle creates a more substantial obstruction in the flow field, resulting in a deceleration of the velocity profile. Further, when the needle's radius is enlarged, it results in a proportional augmentation in the surface area of the needle that interfaces with the fluid. This amplified surface area facilitates enhanced heat transfer efficiency between the needle and its surrounding fluid, consequently elevating the temperature profile surrounding the needle. Conversely, when the needle radius increases, the concentration profile of the fluid diminishes. The cause of this situation stems from the reality that a larger needle radius leads to a greater displacement or expulsion of fluid volume as the needle traverses through it. Consequently, the concentration of the fluid in close proximity to the needle declines as the displaced fluid possesses a lower concentration.

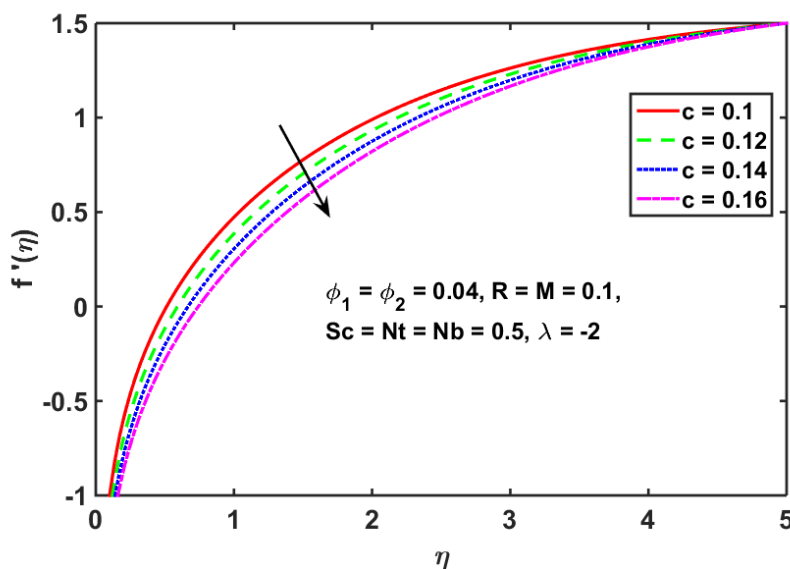


Fig. 10. Nature of $f'(\eta)$ for c

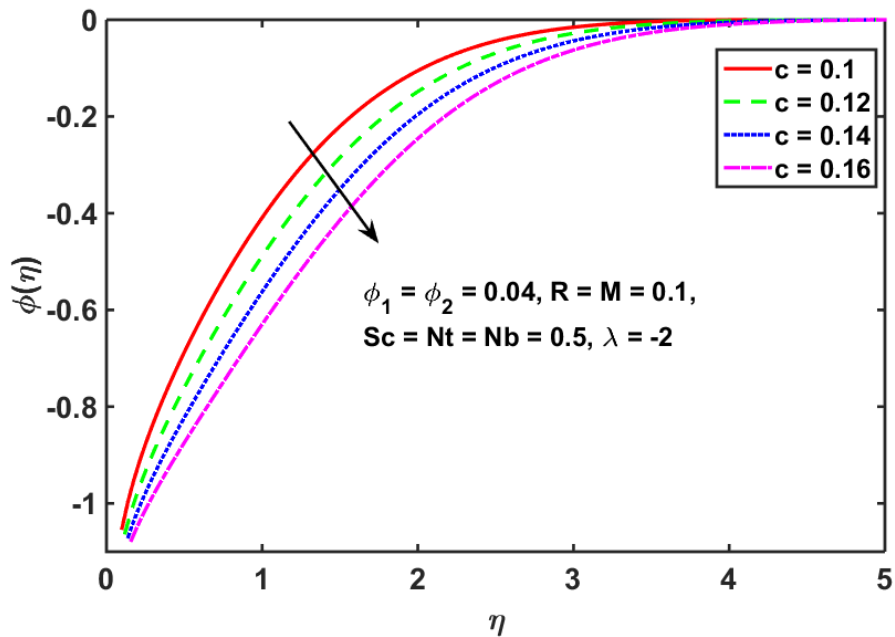


Fig. 11. Nature of $\theta(\eta)$ for c

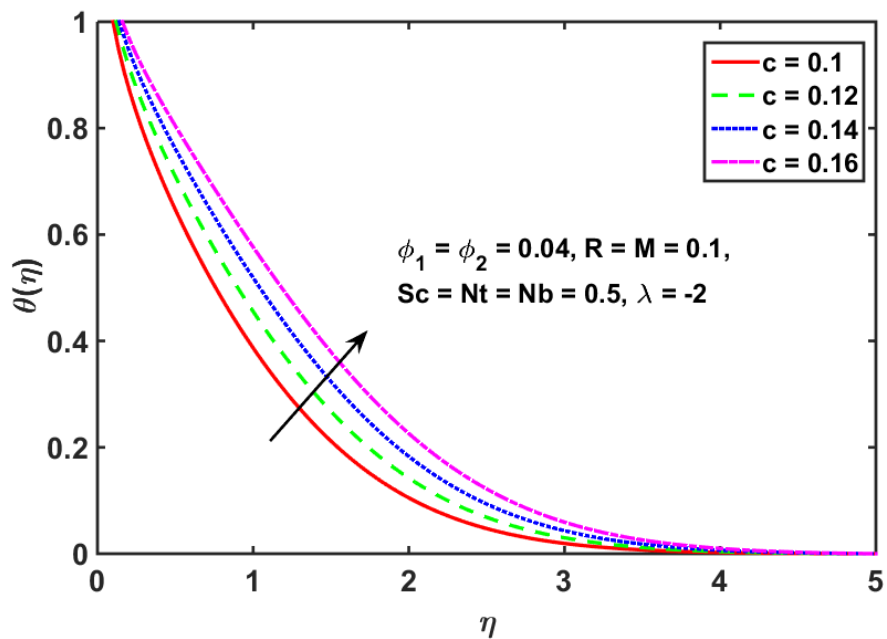


Fig. 12. Nature of $\phi(\eta)$ for c

Figures 13 to 15 demonstrate the effect of the magnetic parameter M on the variations of $f'(\eta)$, $\theta(\eta)$ and $\phi(\eta)$ for the $\text{MgO} - \text{Ag}/\text{H}_2\text{O}$ hybrid nanofluid. With an increasing value of M , there is a decrease observed in both $f'(\eta)$ and $\phi(\eta)$, while $\theta(\eta)$ exhibits an upward trend. Physically, the use of magnetic influences within a flow structure leads to the emergence of a Lorentz force that opposes the flow's direction, resulting in a decrease in velocity as the magnetic parameter is increased. Interestingly, the Lorentz force enhances the transmission of energy in nanoparticles presented in the hybrid nanofluid, which in turn increases the thermal boundary layer, as a result, the thermal characteristics of nanofluid are enhanced. However, the stronger magnetic field also causes the nanoparticles to migrate and accumulate in specific regions of the fluid, leading to a decrease in their concentration in other areas and hence a decline in the concentration distribution of the hybrid nanofluid.

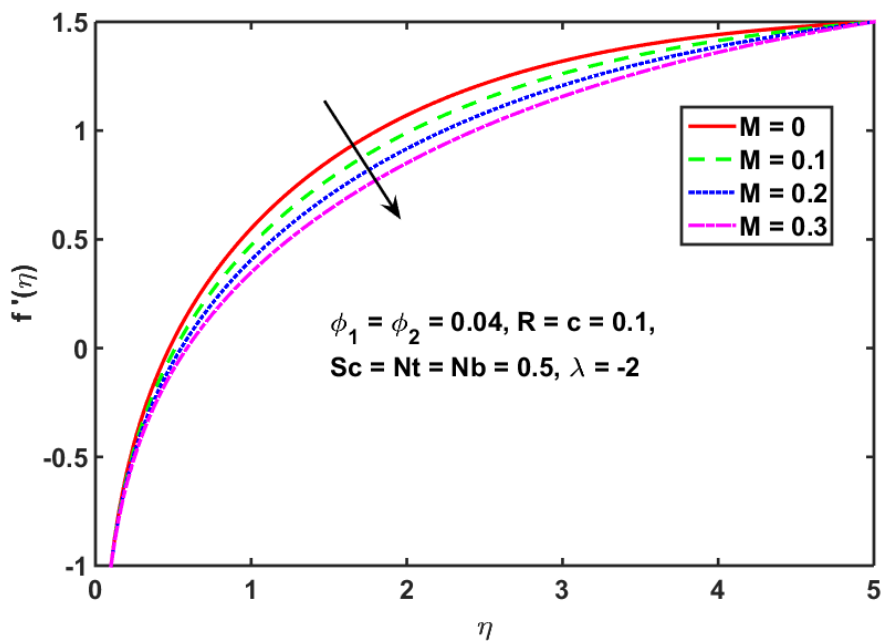


Fig. 13. Nature of $f'(\eta)$ for M

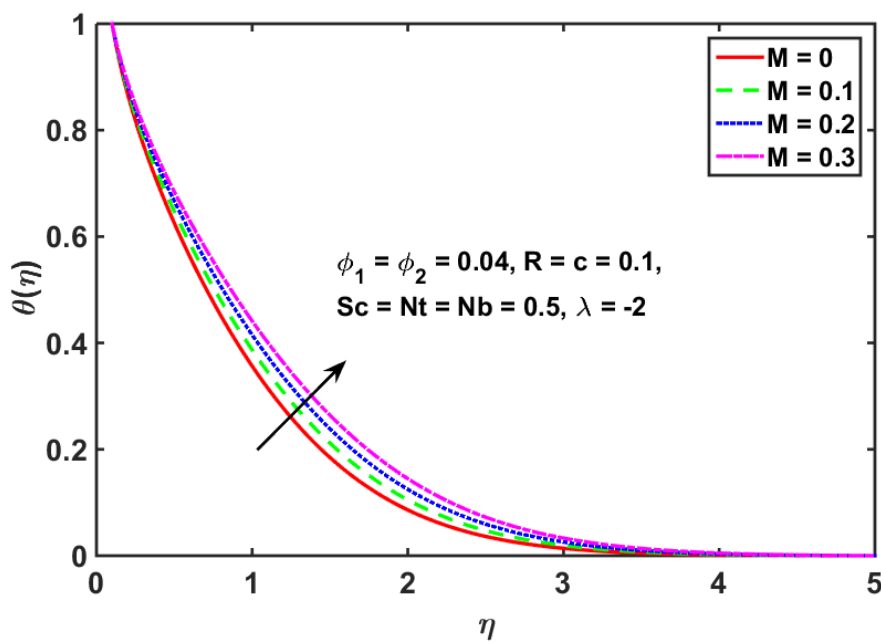


Fig. 14. Nature of $\theta(\eta)$ for M

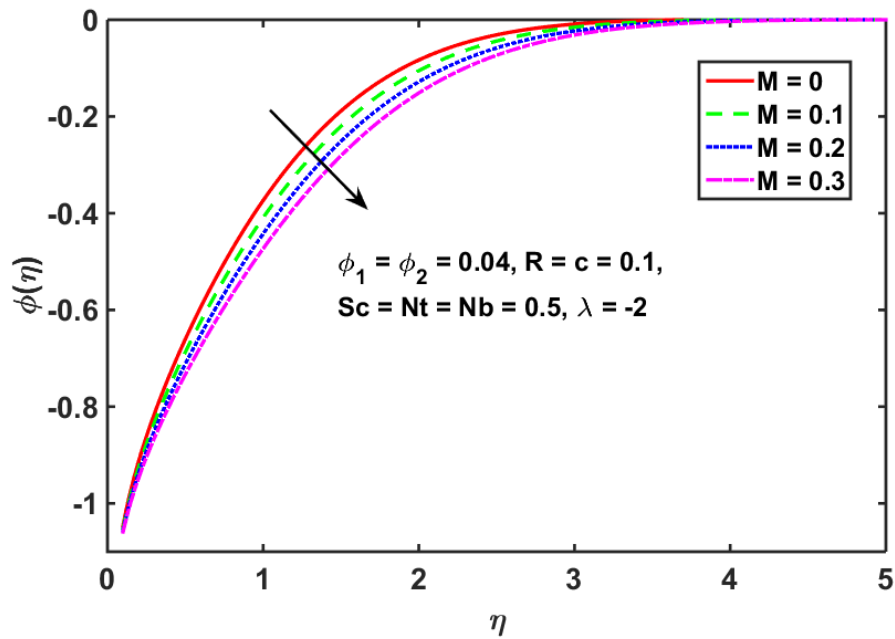


Fig. 15. Nature of $\phi(\eta)$ for M

Figure 16 shows that increasing the radiation parameter (R) in MgO – Ag/H₂O hybrid nanofluid increases the temperature profile $\theta(\eta)$. From a physical standpoint, a higher radiation parameter facilitates the transfer of additional heat into the fluid, consequently amplifying the profile of the temperature and the corresponding boundary layer thickness.

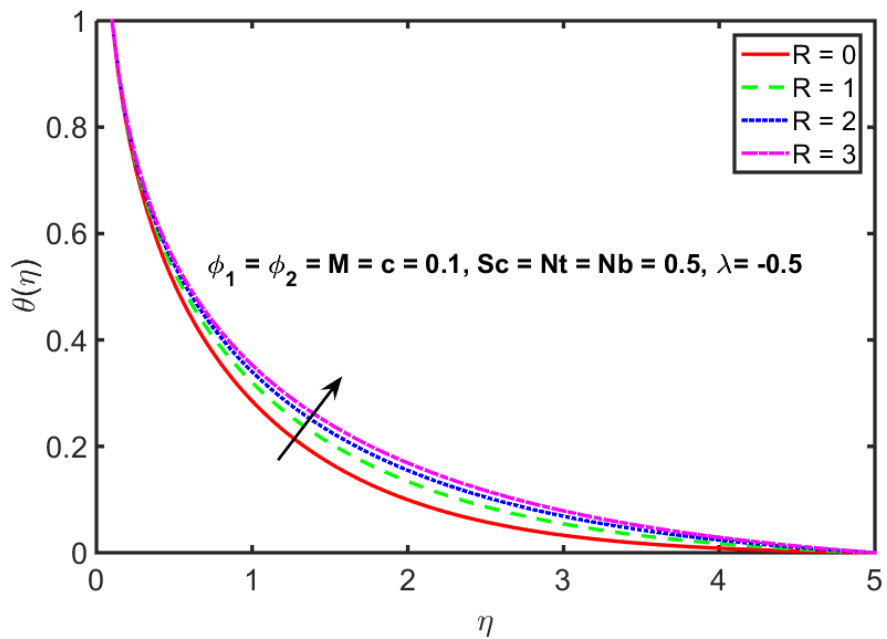


Fig. 16. Nature of $\theta(\eta)$ for R

As the Prandtl number (Pr) increases, the mass and thermal diffusivities of the nanoparticles decrease. This results a reduction in the fluid's thermal characteristics, which is evident in the decrease of $\theta(\eta)$ as shown in Figure 17.

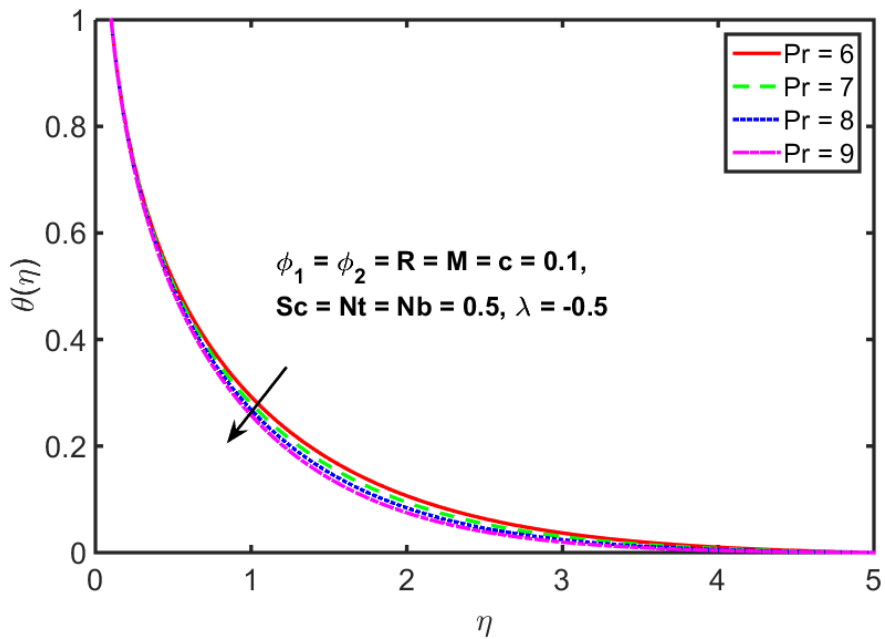


Fig. 17. Nature of $\theta(\eta)$ for Pr

Figures 18 and 19 illustrate how variations in the Schmidt number (Sc) affect the temperature profile and concentration distribution for the MgO – Ag/H₂O hybrid nanofluid. The findings indicate a consistent decrease in both distributions as Sc increases. Increasing the Schmidt number not only hampers fluid mixing but also diminishes the effectiveness of heat transfer, resulting in a decrease in temperature profile. Furthermore, it induces a reduction in the concentration boundary layer, resulting in a deterioration of the concentration properties of nanofluid.

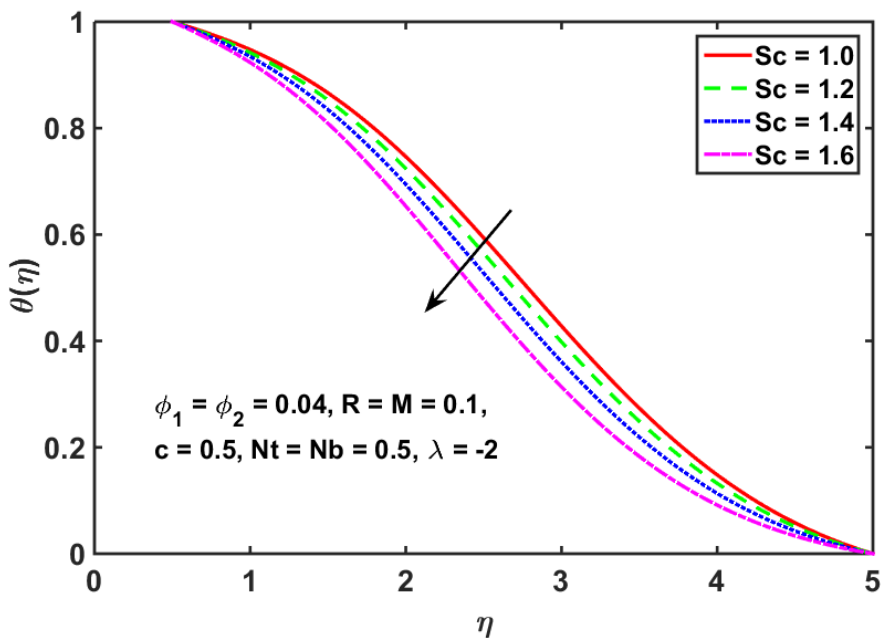


Fig. 18. Nature of $\theta(\eta)$ for Sc

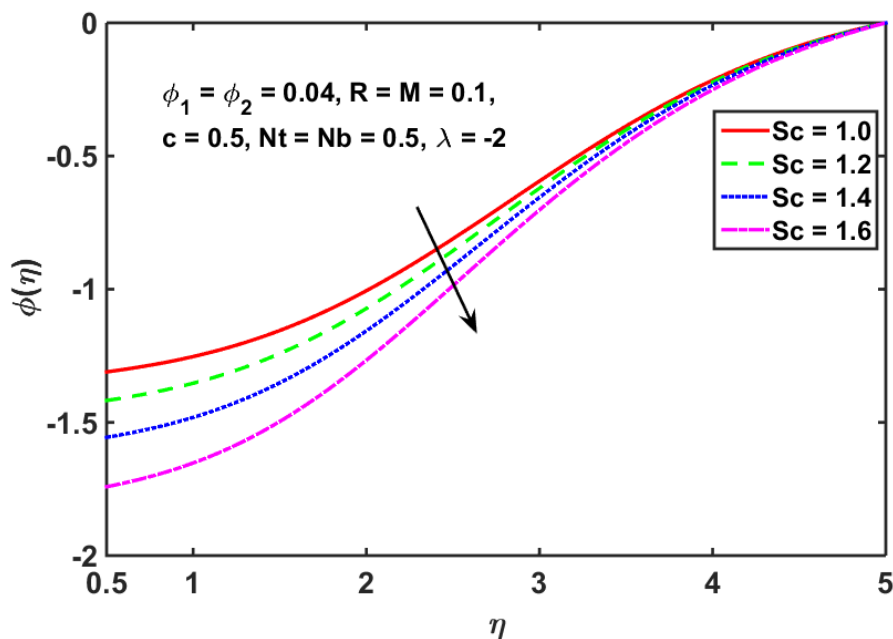


Fig. 19. Nature of $\phi(\eta)$ for Sc

The significance of skin friction coefficient, local Nusselt number and local Sherwood number is paramount in the realms of fluid dynamics as well as heat and mass transfer, shaping diverse aspects of these fields. They empower engineers and scientists to optimize designs, enhance efficacy and gain deeper insights into the fluid dynamics and heat/mass transfer phenomena across a diverse array of fields, including aerospace and automotive engineering, boundary layer analysis, turbulence characterization, heat/mass exchange, cooling systems, natural convection, environmental engineering and biomedical innovations.

While calculating $f''(c)$ (skin friction coefficient), $-\theta'(c)$ (local Nusselt number) and $-\phi'(c)$ (local Sherwood number) in Table 3, we have taken $\phi_1 = \phi_2 = R = M = c = 0.1, Nt = Nb = Sc = 0.5, \lambda = -2$. Notice that when one parameter is changed, all other parameters remain unchanged.

Table 3 presents the findings on the influence of the parameters Nt, Nb, λ, c, M, R and Sc on skin friction coefficient, local Nusselt number and local Sherwood number. The results indicate that greater values of λ, c and M correspond to a decline in skin friction. Regarding the local Nusselt number an increase is observed with higher values of Nt, λ, R and Sc , while the opposite trend is noticed for c and M . Additionally, the Sherwood number rises as Nb, c and M increase, while a contrary behavior is noted for Nt, λ, R and Sc .

Table 3

Influences of $f''(c)$, $-\theta'(c)$ and $-\phi'(c)$ for MgO – Ag/H₂O hybrid nanofluid

Nt	Nb	λ	c	M	R	Sc	$4c^{0.5}A_1f''(c)$	$-2c^{0.5}\frac{k_{hnf}}{k_f}\theta'(c)$	$-2c^{0.5}\phi'(c)$
0.3								2.051218	-0.704820
0.4								2.067992	-0.947444
0.5								2.085032	-1.194064
	0.5								-1.194064
	1.0								-0.597032
	1.5								-0.398021
		-3					10.049828	1.324974	-0.758791
		-2.5					9.316667	1.706368	-0.977210
		-2					8.268200	2.085032	-1.194064
			0.1				8.268200	2.085032	-1.194064
			0.12				7.648134	1.816736	-1.040415
			0.14				7.150386	1.600956	-0.916841
				0.1			8.268200	2.085032	-1.194064
				0.2			7.947580	1.990942	-1.140181
				0.3			7.690627	1.907426	-1.092352
					1			2.361093	-1.352160
					2			2.506637	-1.435511
					3			2.586243	-1.481100
						1		2.181646	-1.249393
						1.2		2.224925	-1.274178
						1.4		2.271207	-1.300683

Table 4 displays a comparison of the similarity skin friction coefficient $f''(c)$ for the various values of slim needle's radius for the base fluid (water) case under the conditions $\phi_1 = \phi_2 = \lambda = M = R = Nt = 0, m_1 = m_2 = Nb = 0.0001$ and $m_f = 100gr$. This comparison aligns with prior findings reported by Souayeh *et al.*, [56] and Dinarvand *et al.*, [28]. Hence, the results presented in Table 4 affirm the robust validity and accuracy of our current numerical approach. Hence, it can be affirmed that our algorithm, based on mass principles and designed for hybrid nanofluid systems performs exceptionally effectively in addressing this specific problem.

Table 4

Comparison of $f''(c)$ with Souayeh *et al.*, [56] and Dinarvand *et al.*, [28]

c	Souayeh [56]	Dinarvand [28]	Current Results
0.001	62.16371	62.177002	62.178534
0.01	8.492412	8.492175	8.492217
0.1	1.288801	1.289074	1.289145
0.2	-	0.751938	0.752031

Table 4 displays a comparison of the similarity skin friction coefficient $f''(c)$ for the various values of slim needle's radius for the base fluid (water) case under the conditions $\phi_1 = \phi_2 = \lambda = M = R = Nt = 0, m_1 = m_2 = Nb = 0.0001$ and $m_f = 100gr$. This comparison aligns with prior findings reported by Souayeh *et al.*, [56] and Dinarvand *et al.*, [28]. Hence, the results presented in Table 4 affirm the robust validity and accuracy of our current numerical approach. Hence, it can be affirmed that our algorithm, based on mass principles and designed for hybrid nanofluid systems performs exceptionally effectively in addressing this specific problem.

6. Conclusion

The main intention of this research is to examine the influences of thermophoresis and Brownian motion on a steady state, laminar, magnetohydrodynamic flow along a horizontally moving thin needle that is maintained at an elevated temperature and filled with MgO – Ag/H₂O. The BVP-5C shooting method is used to achieve the study's objectives.

The findings of this research could be applied to the development of hot wire anemometers, shielded thermocouples for wind velocity measurement, solar collectors, heat exchangers, micro scale cooling devices for the purpose of heat removal and high compact and effective microstructure electronic devices. Based on the findings, the subsequent significant inferences are drawn:

- i. The reduction of the velocity profile can be achieved by elevating the parameters c and M . Also, a noteworthy observation arises in the velocity of λ : a decreasing trend is evident within the range of $0 \leq \lambda \leq 1$, while an intriguing dual behaviour is detected for values of $\lambda < 0$.
- ii. The rise in Nt, λ, Pr and Sc values result a decrease in the temperature profile, while an increase in Nb, c, M and R parameters demonstrate an opposite effect on performance.
- iii. The concentration of the hybrid nanofluid shows an upward trend with increasing Nb and λ values, while a reverse pattern is observed for the parameters Nt, c, M and Sc .
- iv. As λ, c and M values increase, skin friction experiences a reduction, while the Nusselt number demonstrates an upward trend with higher values of Nt, λ, R and Sc but exhibits the opposite behavior for c and M . Further, the Sherwood number rises with greater values of Nb, c and M , but it displays a contrasting pattern for Nt, λ, R and Sc .

7. Future Scope

In the coming years, researchers are poised to investigate a wide range of characteristics pertaining to the steady-state MHD laminar hybrid nanofluid flow, which consists of MgO – Ag/H₂O. This comprehensive examination will encompass factors such as chemical reaction, the porosity parameter and the Forchheimer number. These inquiries will be carried out using computational methods with a strong reliance on cutting-edge technologies like Machine Learning and Artificial Intelligence (AI) to uncover complex phenomena within the field of fluid dynamics. Furthermore, this research could be expanded to explore diverse categories of non-Newtonian fluids, delve into tri-hybrid nanofluids and explore intricate techniques for chemical synthesis and deposition among other potential areas of investigation.

Investigating the properties of hybrid nanofluids in controlled thermal environments can provide valuable insights for a range of energy-related applications, including concentrated solar power systems, optimizing heat transfer efficiency, lowering energy consumption and more. A deeper understanding of the underlying principles governing heat transfer and fluid dynamics has the potential to catalyse progress in the creation of more cost-effective and efficient methods for harnessing solar energy. Nevertheless, the integration of nanoparticles at the nanoscale into heat transfer fluids has resulted in substantial improvements in thermal conductivity.

Acknowledgement

This research was not funded by any grant.

References

- [1] Chen, J. L. S., and T. N. Smith. "Forced convection heat transfer from nonisothermal thin needles." (1978): 358-362. <https://doi.org/10.1115/1.3450809>
- [2] Waini, Iskandar, Anuar Ishak, and Ioan Pop. "Flow and heat transfer of a hybrid nanofluid past a permeable moving surface." *Chinese Journal of Physics* 66 (2020): 606-619. <https://doi.org/10.1016/j.cjph.2020.04.024>
- [3] Rammoorthi, Rajakumari, and Dhivya Mohanavel. "Influence of Radiative Magnetic Field on a Convective Flow of a Chemically Reactive Hybrid Nanofluid over a Vertical Plate." *Journal of Advanced Research in Fluid Mechanics and Thermal Sciences* 105, no. 1 (2023): 90-106. <https://doi.org/10.37934/arfmts.105.1.90106>
- [4] Sarfraz, Mahnoor, Masood Khan, and Muhammad Yasir. "Dynamics of water conveying iron oxide and graphene nanoparticles subject to stretching/spiraling surface: An asymptotic approach." *Ain Shams Engineering Journal* 14, no. 8 (2023): 102021. <https://doi.org/10.1016/j.asej.2022.102021>
- [5] Khan, Umair, Anum Shafiq, A. Zaib, and Dumitru Baleanu. "Hybrid nanofluid on mixed convective radiative flow from an irregular variably thick moving surface with convex and concave effects." *Case Studies in Thermal Engineering* 21 (2020): 100660. <https://doi.org/10.1016/j.csite.2020.100660>
- [6] Arulmozhi, S., K. Sukkiramathi, Shyam Sundar Santra, R. Edwan, Unai Fernandez-Gamiz, and Samad Noeiaghdam. "Heat and mass transfer analysis of radiative and chemical reactive effects on MHD nanofluid over an infinite moving vertical plate." *Results in Engineering* 14 (2022): 100394. <https://doi.org/10.1016/j.rineng.2022.100394>
- [7] Thirupathi, Gurralla, Kamatam Govardhan, and Ganji Narender. "Radiative magnetohydrodynamics Casson nanofluid flow and heat and mass transfer past on nonlinear stretching surface." *Journal of Advanced Research in Numerical Heat Transfer* 6, no. 1 (2021): 1-21. <https://doi.org/10.3762/bxiv.2021.65.v1>
- [8] Alkasasbeh, Hamzeh. "Numerical solution of heat transfer flow of casson hybrid nanofluid over vertical stretching sheet with magnetic field effect." *CFD Letters* 14, no. 3 (2022): 39-52. <https://doi.org/10.37934/cfdl.14.3.3952>
- [9] Rai, Purnima, and Upendra Mishra. "Numerical Simulation of Boundary Layer Flow Over a Moving Plate in The Presence of Magnetic Field and Slip Conditions." *Journal of Advanced Research in Fluid Mechanics and Thermal Sciences* 95, no. 2 (2022): 120-136.
- [10] Dharmiaiah, G., JL Rama Prasad, K. S. Balamurugan, I. Nurhidayat, Unai Fernandez-Gamiz, and Samad Noeiaghdam. "Performance of magnetic dipole contribution on ferromagnetic non-Newtonian radiative MHD blood flow: An application of biotechnology and medical sciences." *Heliyon* 9, no. 2 (2023). <https://doi.org/10.1016/j.heliyon.2023.e13369>
- [11] Manvi, Bharatkumar, Jagadish Tawade, Mahadev Biradar, Samad Noeiaghdam, Unai Fernandez-Gamiz, and VEDIYAPPAN GOVINDAN. "The effects of MHD radiating and non-uniform heat source/sink with heating on the momentum and heat transfer of Eyring-Powell fluid over a stretching." *Results in Engineering* 14 (2022): 100435. <https://doi.org/10.1016/j.rineng.2022.100435>
- [12] Madhura, K. R., Babitha, and S. S. Iyengar. "Impact of heat and mass transfer on mixed convective flow of nanofluid through porous medium." *International Journal of Applied and Computational Mathematics* 3, no. Suppl 1 (2017): 1361-1384. <https://doi.org/10.1007/s40819-017-0424-3>
- [13] Sarfraz, Mahnoor, and Masood Khan. "Heat transfer efficiency in planar and axisymmetric ternary hybrid nanofluid flows." *Case Studies in Thermal Engineering* 44 (2023): 102857. <https://doi.org/10.1016/j.csite.2023.102857>
- [14] Sarfraz, Mahnoor, and Masood Khan. "Magnetized homann flow comprising GO and Co3O4 nanoparticles past a biaxially stretching surface." *Physica Scripta* 98, no. 3 (2023): 035218. <https://doi.org/10.1088/1402-4896/acba61>
- [15] Sarfraz, Mahnoor, and Masood Khan. "Thermodynamic irreversibility analysis of water conveying argentine and titania nanoparticles subject to inclined stretching surface." *Physica Scripta* 98, no. 2 (2023): 025205. <https://doi.org/10.1088/1402-4896/acab92>
- [16] Maheswari, Chundru, Ravuri Mohana Ramana, Shaik Mohiddin Shaw, G. Dharmiaiah, and S. Noeiaghdam. "Numerical investigation on MHD forchheimer flow of Fe3O4-H2O, Cu-H2O and Ag-H2O nanofluids over permeable stretching sheet with radiation." *Results in Engineering* (2023): 101194.
- [17] Babitha, K. R. Madhura, and S. S. Iyengar. "An investigation of Heat Transfer and Magnetohydrodynamics Flow of Fractional Oldroyd-B Nanofluid Suspended with Carbon Nanotubes." *International Journal of Applied and Computational Mathematics* 8, no. 3 (2022): 133. <https://doi.org/10.1007/s40819-022-01330-4>
- [18] Anitha, L., B. J. Gireesha, and M. L. Keerthi. "Irreversibility analysis of tangent hyperbolic fluid flow in a microchannel: a hybrid nanoparticles aspects." *Physica Scripta* 98, no. 3 (2023): 035220. <https://doi.org/10.1088/1402-4896/acba53>
- [19] Sarfraz, Mahnoor, and Masood Khan. "Entropy generation analysis of CNT-based nanofluid flows induced by a moving plate." *ZAMM-Journal of Applied Mathematics and Mechanics/Zeitschrift für Angewandte Mathematik und Mechanik* (2023): e202200555. <https://doi.org/10.1002/zamm.202200555>

- [20] Guled, C. N., J. V. Tawade, P. Kumam, S. Noeiaghdam, I. Maharudrappa, S. M. Chithra, and V. Govindan. "The heat transfer effects of MHD slip flow with suction and injection and radiation over a shrinking sheet by optimal homotopy analysis method." *Results in Engineering* 18 (2023): 101173. <https://doi.org/10.1016/j.rineng.2023.101173>
- [21] Salleh, Siti Nur Alwani, Norfifah Bachok, Norihan Md Arifin, and Fadzilah Md Ali. "Effect of Buoyancy Force on The Flow and Heat Transfer Around a Thin Needle in Al O-Cu 2 3 Hybrid Nanofluid." *CFD Letters* 12, no. 1 (2020): 22-36. <https://doi.org/10.3390/sym12071176>
- [22] Khan, Ziad, Hari Mohan Srivastava, Pshtiwan Othman Mohammed, Muhammad Jawad, Rashid Jan, and Kamsing Nonlaopon. "Thermal boundary layer analysis of MHD nanofluids across a thin needle using non-linear thermal radiation." *Mathematical Biosciences and Engineering* 19, no. 12 (2022): 14116-14141. <https://doi.org/10.3934/mbe.2022658>
- [23] Waini, Iskandar, Anuar Ishak, and Ioan Pop. "Hybrid nanofluid flow and heat transfer past a vertical thin needle with prescribed surface heat flux." *International Journal of Numerical Methods for Heat & Fluid Flow* 29, no. 12 (2019): 4875-4894. <https://doi.org/10.1108/HFF-04-2019-0277>
- [24] Lee, Lawrence L. "Boundary layer over a thin needle." *The physics of fluids* 10, no. 4 (1967): 820-822. <https://doi.org/10.1063/1.1762194>
- [25] Narain, Jai Prakash, and Mahinder S. Uberoi. "Forced heat transfer over thin needles." (1972): 240-242. <https://doi.org/10.1115/1.3449910>
- [26] Narain, J. P., and M. S. Uberoi. "Free-convection heat transfer from a thin vertical needle." *Phys. Fluids* 15 (1972): 928-929. <https://doi.org/10.1063/1.1694001>
- [27] Narain, Jai Prakash, and Mahinder S. Uberoi. "Combined forced and free-convection heat transfer from vertical thin needles in a uniform stream." *The Physics of Fluids* 15, no. 11 (1972): 1879-1882. <https://doi.org/10.1063/1.1693798>
- [28] Dinarvand, Saeed, Seyed Mehdi Mousavi, Mohammad Yousefi, and Mohammadreza Nademi Rostami. "MHD flow of MgO-Ag/water hybrid nanofluid past a moving slim needle considering dual solutions: An applicable model for hot-wire anemometer analysis." *International Journal of Numerical Methods for Heat & Fluid Flow* 32, no. 2 (2022): 488-510. <https://doi.org/10.1108/HFF-01-2021-0042>
- [29] Tlili, Iskander, Hossam A. Nabwey, M. Girinath Reddy, N. Sandeep, and Maddileti Pasupula. "Effect of resistive heating on incessantly poignant thin needle in magnetohydrodynamic Sakiadis hybrid nanofluid." *Ain Shams Engineering Journal* 12, no. 1 (2021): 1025-1032. <https://doi.org/10.1016/j.asej.2020.09.009>
- [30] Jahan, Sultana, M. Ferdows, M. D. Shamshuddin, and Khairy Zaimi. "Effects of solar radiation and viscous dissipation on mixed convective non-isothermal hybrid nanofluid over moving thin needle." *Journal of Advanced Research in Micro and Nano Engineering* 3, no. 1 (2021): 1-11.
- [31] Waini, Iskandar, Anuar Ishak, and Ioan Pop. "Hybrid nanofluid flow and heat transfer past a vertical thin needle with prescribed surface heat flux." *International Journal of Numerical Methods for Heat & Fluid Flow* 29, no. 12 (2019): 4875-4894. <https://doi.org/10.1108/HFF-04-2019-0277>
- [32] Arshad, Mubashar, Ali Hassan, Qusain Haider, Fahad M. Alharbi, Najah Alsubaie, Abdullah Alhushaybari, Diana-Petronela Burduhos-Nergis, and Ahmed M. Galal. "Rotating hybrid nanofluid flow with chemical reaction and thermal radiation between parallel plates." *Nanomaterials* 12, no. 23 (2022): 4177. <https://doi.org/10.3390/nano12234177>
- [33] Kumar, Y. Suresh, Y. Madhavi Reddy, Siva Mala Munnangi, and Srinivasa Rao Puchakayala. "Effects of Activation Energy Diffusion Thermo and Nonlinear Thermal Radiation on Mixed Convection Casson Fluid Flow Through a Vertical Cone with Porous Media in the Presence of Brownian Motion and Thermophoresis." *Journal of Advanced Research in Fluid Mechanics and Thermal Sciences* 108, no. 1 (2023): 75-92. <https://doi.org/10.37934/arfmts.108.1.7592>
- [34] Reddy, Y., M. Suryanarayana Reddy, P. Sudarsana Reddy, and Ali J. Chamkha. "Effect of Brownian motion and thermophoresis on heat and mass transfer flow over a horizontal circular cylinder filled with nanofluid." *Journal of Nanofluids* 6, no. 4 (2017): 702-710. <https://doi.org/10.1166/jon.2017.1365>
- [35] Gopalam, Neeraja, and Saila Kumari Annareddy. "Hall Current and Thermal Radiation Effects on MHD Nanofluid in the Presence of Heat Source/Sink, Brownian Motion and Thermophoresis with Inclined Plates." *Journal of Advanced Research in Fluid Mechanics and Thermal Sciences* 104, no. 1 (2023): 152-168. <https://doi.org/10.37934/arfmts.104.1.152168>
- [36] Vaddemani, Ramachandra Reddy, Sreedhar Ganta, and Raghunath Kodi. "Effects of Hall Current, Activation Energy and Diffusion Thermo of MHD Darcy-Forchheimer Casson Nanofluid Flow in the Presence of Brownian Motion and Thermophoresis." *Journal of Advanced Research in Fluid Mechanics and Thermal Sciences* 105, no. 2 (2023): 129-145. <https://doi.org/10.37934/arfmts.105.2.129145>

- [37] Almeida, Felicita, Bijjanal Jayanna Gireesha, and Puttaswamy Venkatesh. "Magnetohydrodynamic flow of a micropolar nanofluid in association with Brownian motion and thermophoresis: Irreversibility analysis." *Heat Transfer* 52, no. 2 (2023): 2032-2055. <https://doi.org/10.1002/htj.22773>
- [38] Madhura, K. R., and Babitha. "Numerical study on magnetohydrodynamics micropolar Carreau nanofluid with Brownian motion and thermophoresis effect." *International Journal of Modelling and Simulation* (2023): 1-14. <https://doi.org/10.1080/02286203.2023.2234240>
- [39] Mohammed, Abdur Raheem, Mohiddin shaw Shaik, Mohana Ramana Ravuri, Maheswari Ch, and Dharmiaiah Gurram. "Thermophoresis, Brownian Diffusion, Porosity, and Magnetic Parameters' Effects on Three-Dimensional Rotating Ag-CuO/H₂O Hybrid Nanofluid Flow across a Linearly Stretched Sheet with Aligned Magnetic Field." *CFD Letters* 15, no. 10 (2023): 123-151. <https://doi.org/10.37934/cfdl.15.10.123151>
- [40] Madhukesh, J. K., G. K. Ramesh, M. D. Alsulami, and B. C. Prasannakumara. "Characteristic of thermophoretic effect and convective thermal conditions on flow of hybrid nanofluid over a moving thin needle." *Waves in Random and Complex Media* (2021): 1-23. <https://doi.org/10.1080/17455030.2021.2012303>
- [41] Waini, Iskandar, Anuar Ishak, and Ioan Pop. "Hybrid nanofluid flow past a permeable moving thin needle." *Mathematics* 8, no. 4 (2020): 612. <https://doi.org/10.3390/math8040612>
- [42] Jahan, Sultana, M. Ferdows, Md Shamshuddin, and Khairy Zaimi. "Radiative mixed convection flow over a moving needle saturated with non-isothermal hybrid nanofluid." *Journal of Advanced Research in Fluid Mechanics and Thermal Sciences* 88, no. 1 (2021): 81-93. <https://doi.org/10.37934/arfmts.88.1.8193>
- [43] Khan, Arshad, Wiyada Kumam, Imran Khan, Anwar Saeed, Taza Gul, Poom Kumam, and Ishtiaq Ali. "Chemically reactive nanofluid flow past a thin moving needle with viscous dissipation, magnetic effects and hall current." *Plos one* 16, no. 4 (2021): e0249264. <https://doi.org/10.1371/journal.pone.0249264>
- [44] Khan, Arshad, Anwar Saeed, Asifa Tassaddiq, Taza Gul, Poom Kumam, Ishtiaq Ali, and Wiyada Kumam. "Bio-convective and chemically reactive hybrid nanofluid flow upon a thin stirring needle with viscous dissipation." *Scientific reports* 11, no. 1 (2021): 8066. <https://doi.org/10.1038/s41598-021-86968-8>
- [45] Waini, Iskandar, Anuar Ishak, and Ioan Pop. "On the stability of the flow and heat transfer over a moving thin needle with prescribed surface heat flux." *Chinese Journal of Physics* 60 (2019): 651-658. <https://doi.org/10.1016/j.cjph.2019.06.008>
- [46] Esfe, Mohammad Hemmat, Ali Akbar Abbasian Arani, Mohammad Rezaie, Wei-Mon Yan, and Arash Karimipour. "Experimental determination of thermal conductivity and dynamic viscosity of Ag-MgO/water hybrid nanofluid." *International Communications in Heat and Mass Transfer* 66 (2015): 189-195. <https://doi.org/10.1016/j.icheatmasstransfer.2015.06.003>
- [47] Soid, Siti Khuzaimah, Anuar Ishak, and Ioan Pop. "Boundary layer flow past a continuously moving thin needle in a nanofluid." *Applied Thermal Engineering* 114 (2017): 58-64. <https://doi.org/10.1016/j.applthermaleng.2016.11.165>
- [48] Tiwari, Raj Kamal, and Manab Kumar Das. "Heat transfer augmentation in a two-sided lid-driven differentially heated square cavity utilizing nanofluids." *International Journal of heat and Mass transfer* 50, no. 9-10 (2007): 2002-2018. <https://doi.org/10.1016/j.ijheatmasstransfer.2006.09.034>
- [49] Daniel, Yahaya Shagaiya, and Simon K. Daniel. "Effects of buoyancy and thermal radiation on MHD flow over a stretching porous sheet using homotopy analysis method." *Alexandria Engineering Journal* 54, no. 3 (2015): 705-712. <https://doi.org/10.1016/j.aej.2015.03.029>
- [50] Dinarvand, Saeed, Mohammadreza Nademi Rostami, and Ioan Pop. "A novel hybridity model for TiO₂-CuO/water hybrid nanofluid flow over a static/moving wedge or corner." *Scientific reports* 9, no. 1 (2019): 16290. <https://doi.org/10.1038/s41598-019-52720-6>
- [51] Dinarvand, Saeed, Mohammadreza Nademi Rostami, Rassoul Dinarvand, and Ioan Pop. "Improvement of drug delivery micro-circulatory system with a novel pattern of CuO-Cu/blood hybrid nanofluid flow towards a porous stretching sheet." *International Journal of Numerical Methods for Heat & Fluid Flow* 29, no. 11 (2019): 4408-4429. <https://doi.org/10.1108/HFF-01-2019-0083>
- [52] Sundar, L. Syam, Korada Viswanatha Sharma, Manoj K. Singh, and A. C. M. Sousa. "Hybrid nanofluids preparation, thermal properties, heat transfer and friction factor—a review." *Renewable and Sustainable Energy Reviews* 68 (2017): 185-198. <https://doi.org/10.1016/j.rser.2016.09.108>
- [53] Hamid, Aamir, Abdul Hafeez, Masood Khan, A. S. Alshomrani, and Metib Alghamdi. "Heat transport features of magnetic water-graphene oxide nanofluid flow with thermal radiation: Stability Test." *European Journal of Mechanics-B/Fluids* 76 (2019): 434-441. <https://doi.org/10.1016/j.euromechflu.2019.04.008>
- [54] Dinarvand, S. A. E. E. D., and M. Nademi Rostami. "Mixed convection of a Cu-Ag/water hybrid nanofluid along a vertical porous cylinder via modified Tiwari-Das model." *J. Theor. Appl. Mech* 49 (2019): 149-169. <https://doi.org/10.7546/JTAM.49.19.02.05>

- [55] Sabour, M., Mohammad Ghalambaz, and Ali Chamkha. "Natural convection of nanofluids in a cavity: criteria for enhancement of nanofluids." *International Journal of Numerical Methods for Heat & Fluid Flow* 27, no. 7 (2017): 1504-1534. <https://doi.org/10.1108/HFF-12-2015-0516>
- [56] Souayeh, Basma, M. Ganeswara Reddy, P. Sreenivasulu, T. M. I. M. Poornima, Mohammad Rahimi-Gorji, and Ibrahim M. Alarifi. "Comparative analysis on non-linear radiative heat transfer on MHD Casson nanofluid past a thin needle." *Journal of Molecular Liquids* 284 (2019): 163-174. <https://doi.org/10.1016/j.molliq.2019.03.151>